JOURNAL OF Applied Polymer SCIENCE

Self-Crosslinkable Lignin/Epoxidized Natural Rubber Composites

Can Jiang, Hui He, Xiaojie Yao, Peng Yu, Ling Zhou, Demin Jia
Department of Polymer Materials and Engineering, South China University of Technology, Guangzhou 510640, People's Republic of China
Correspondence to: H. He (E-mail: pshuihe@scut.edu.cn)

ABSTRACT: Self-crosslinkable lignin/epoxidized natural rubber composites (SLEs) were prepared through a high-temperature dynamic heat treatment procedure followed by a postcuring process. Because of the ring-opening reaction between lignin and epoxidized natural rubber (ENR), lignin as a crosslinker and reinforcing filler was uniformly dispersed into the ENR matrix and was highly compatible with the polymer matrix; this was confirmed by scanning electron microscopy. The curing behavior, mechanical properties, and dynamic mechanical properties of the SLEs were studied. The results show that the crosslinking degree, glass-transition temperature, modulus, and tensile properties of the SLEs substantially increased with the addition of lignin. A physical model was used to verify the strong interactions between lignin and ENR. Stress–strain curves and X-ray diffraction suggested that the reinforcement effect on the SLEs mainly originated from lignin itself rather than from strain-induced crystallization. © 2014 Wiley Periodicals, Inc. J. Appl. Polym. Sci. **2014**, *131*, 41166.

KEYWORDS: biomaterials; cellulose and other wood products; composites; crosslinking; rubber

Received 23 April 2014; accepted 13 June 2014
DOI: 10.1002/app.41166

INTRODUCTION

Epoxidized natural rubber (ENR) is a modified natural rubber and retains most of its properties. In particular, ENR is still able to generate strain-induced crystallization up to a 50 mol % epoxidation level.[1] However, compared with its native natural rubber counterpart, ENR exhibits various additional advantages, such as a good oil resistance,[2] low gas permeability,[3] good adhesive ability, and enhanced compatibility.[4,5] In addition, the epoxy groups of ENR are randomly distributed along the polymer backbone and can readily react with many nucleophilic reagents for further modification or crosslinking.[6–9] Previous studies have shown that ENR can be crosslinked by difunctional or multifunctional amines or acids via the ring opening of the epoxy groups in the presence of catalysts (phenol or bisphenol A for amines and imidazole for acids).[10,11] Unfortunately, the ultimate mechanical properties of those amine- or acid-crosslinked ENRs are still at low levels. This has mainly been ascribed to the fact that the amine– or acid–ENR network is relatively rigid and is not as stretchable as the sulfur–ENR one; this, thereby hinders strain-induced crystallization.[11] Despite the rigid network formed by the ring-opening reaction, the properties of amine- or acid-crosslinked ENR can be significantly improved by the loading of reinforcing fillers, such as carbon black[12] and silica,[13] into the rubber matrix.

In this study, lignin was used not only as a crosslinker to cure ENR but also as a reinforcing filler to improve the performance of lignin/ENR composites. Lignin is a renewable and biodegradable aromatic polymer that is mainly obtained as a byproduct in the pulping industry. It consists of three phenyl propanoid units, *p*-hydroxyphenyl, guaiacyl, and syringyl, which are attached to one another by a series of characteristic linkages (β-O-4, β-5, β-β, etc.).[14] The chemical functional groups in the lignin molecule include hydroxyl (aliphatic hydroxyl and phenolic hydroxyl), methoxyl, carbonyl, and carboxyl groups in various amounts and proportions,[15] in which the hydroxyl and carboxyl groups can react with the epoxy sites of the ENR; this makes lignin become the crosslinking center of the lignin/ENR composites, as illustrated in Figure 1.

Although there have been a large amount of studies on the incorporation of lignin into rubber-based materials[16–18] or epoxy resins[19,20] to maximize the value of lignin, no reports of lignin–ENR composites, especially with the use of lignin as a crosslinker and reinforcing filler for ENR, have been done so far. Herein, we made an attempt to study the influence of the lignin content ($[L]$) and curing time on the ring-opening reaction and mechanical performance of ENR. The interface interactions between lignin and the ENR matrix and the confinement effect of lignin toward ENR molecular chains were also examined in detail by dynamic mechanical analysis (DMA). The reinforcement mechanism of the self-crosslinkable lignin/epoxidized natural rubber composites (SLEs) was carefully studied through its stress–strain properties and X-ray diffraction (XRD) measurements.

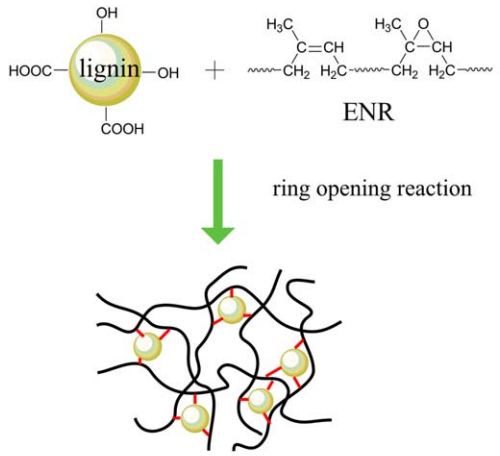

Figure 1. Schematic illustration of the preparation process for the SLEs. [Color figure can be viewed in the online issue, which is available at wileyonlinelibrary.com.]

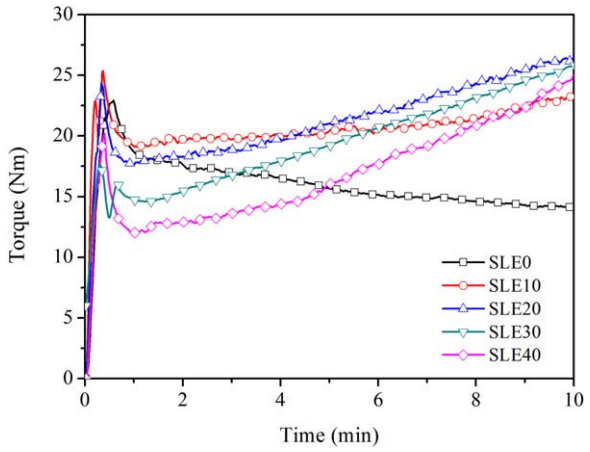

Figure 2. Haake S' curves for the pure ENR, SEL10, SEL20, SEL30, and SEL40 during an HTDHT procedure at 180°C. [Color figure can be viewed in the online issue, which is available at wileyonlinelibrary.com.]

EXPERIMENTAL

Materials

ENR, containing 25 mol % epoxy groups, was purchased from the Tropical Crops Research Center of Zhanjiang (China). Lignin (industrial sulfate lignin), with an average molecular weight of 3801 and a polydispersity index of 2.15, was purchased from Tralin Paper Co., Ltd. (Shandong, China).

Sample Preparation

Before use, lignin was purified as previously described.[21] First, 10 wt % water was added to the purified lignin. Subsequently, different desired amounts of lignin (10, 20, 30, and 40 phr) were mixed with 100-phr ENR in an open two-roll mill. This was followed by a high-temperature dynamic heat treatment (HTDHT) procedure, that is, sealing in a Haake Polylab mixer with a rotation speed of 60 rpm at 180°C for 10 min. No other rubber additives were incorporated into the composites. Then, the resulting mixtures were cured in a standard mold at 180°C. The 0-, 10-, 20-, 30-, and 40-phr lignin-filled ENR composites were designated as SLE0, SLE10, SLE20, SLE30, and SLE40, respectively.

Characterization

The HTDHT procedure was carried out on a Haake torque rheometer (HAAKE400P, Germany). The corresponding torque (S') curves were recorded. The curing curves of the SLEs at 180°C were monitored by an oscillating disk rheometer (U-CAN UR-2030 vulcameter, Taiwan). Scanning electron micrographs of the composites were taken with a Nova NanoSEM 430 instrument (FEI, The Netherlands) at an acceleration voltage of 10 kV. The fracture surface was obtained by the splitting of the bulk sample, which was quenched in liquid nitrogen. Before the observation, a thin layer of gold was evaporated on the fractured surface. The crosslinking densities of the SLEs were determined by the NMR method, and the measurements were performed on an XLDS-15 NMR crosslinking density analyzer (IIC Innovative Imaging Crop, KG). To measure the mechanical properties, dumbbell-shaped specimens were cut from molded rubber sheets to measure the tensile properties. The modulus, tensile strength, and elongation at break were determined from stress–strain curves obtained from a tensile instrument (U-CAN UT-2060, Taiwan) at room temperature according to the procedure described in ASTM D 412. The DMA spectra of the samples were obtained with a DMA 242D dynamic mechanical analyzer (Netzsch Co., Germany). Specimens with sizes of 30 × 6 × 2 mm^3 were analyzed in tensile mode at a constant frequency of 1 Hz, a strain of 0.5%, and a temperature ranging from −100 to 80°C at a heating rate of 3°C/min. XRD experiments were conducted at ambient temperature on a Rigaku Dmax/III diffractometer (Rigaku Corp., Tokyo, Japan) with Cu Kα radiation (Wavelength $\lambda = 1.54$ Å). The generator was operated at 40 kV and 30 mA. The samples under the stretching state in a homemade mold were scanned from 5 to 30° with a step length of 0.04°.

RESULTS AND DISCUSSION

HTDHT

It has been widely accepted that lignin as a dry powder mixed in a straightforward manner into rubber shows almost no reinforcing effects.[22] This is believed to be a result of the lignin particles adhering together by hydrogen bonding[23] and thus not being dispersed into the rubber through mixing at a normal temperatures. As a thermoplastic material, lignin exhibits its glass-transition temperature (T_g) in a wide range, about 60–190°C, depending on the species, applied extraction processes, low-molecular-weight contaminants (including water and solvents), and so on.[24–27] In particular, a small amount of water can markedly lower the T_g of lignin by breaking the hydrogen bonds between the lignin particles.[27] Therefore, in our study, lignin containing 10 wt % water was readily softened and crushed into small pieces under a high temperature and shear force. Simultaneously combining the ring-opening reaction with ENR, we further disaggregated and wrapped the particles by ENR, thus preventing the fine lignin particles from fusing together again. The reaction between lignin and ENR during the HTDHT procedure was indirectly confirmed by the Haake S'. As shown in Figure 2, the Haake S' of the pure ENR

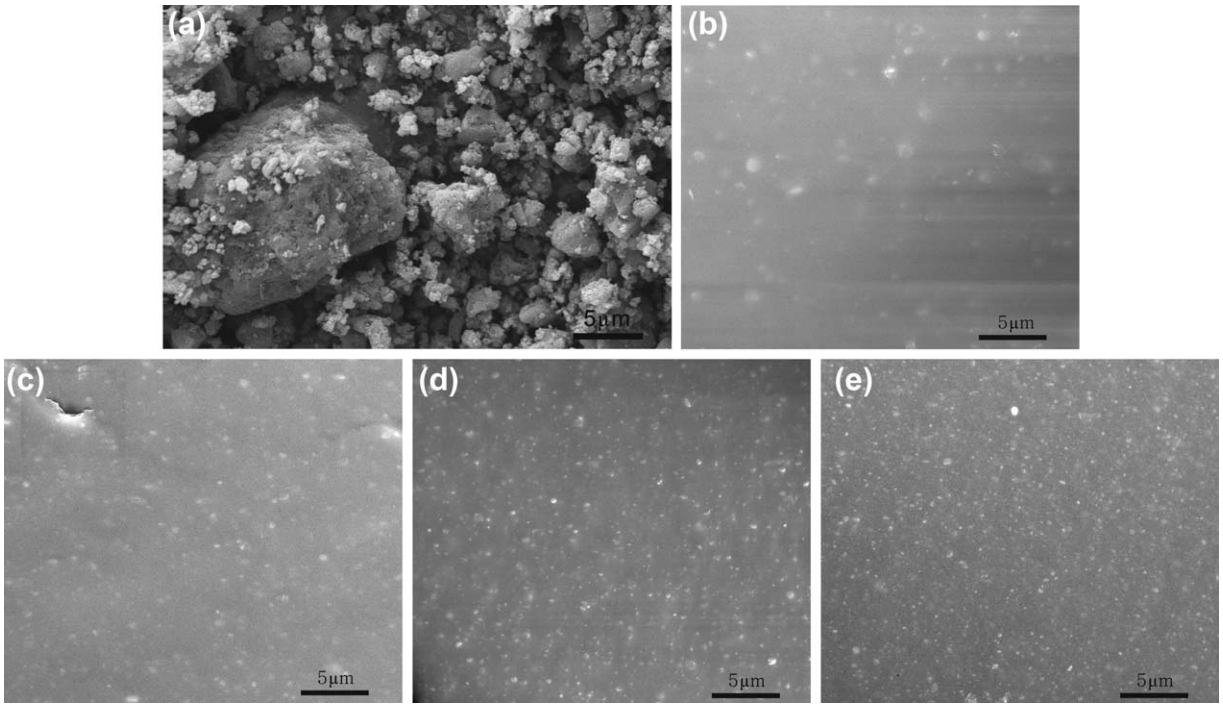

Figure 3. SEM photos of (a) dry lignin powder, (b) SLE10, (c) SLE20, (d) SLE30, and (e) SLE40.

significantly decreased with increasing time, mainly because of the chain scission of the ENR macromolecules under high temperature. In contrast, the S' of the lignin-filled ENR composites was substantially increased; this sufficiently verified the ring-opening reaction between lignin and ENR. Moreover, the increase in S' seemed to be more obvious with increasing $[L]$; this indicated that when more lignin was added, a higher reaction rate was achieved. Despite the crosslinking of the SLEs in the HTDHT, the network structures were still not integrated enough with the SLEs to obtain the available mechanical properties. Therefore, a postcuring process was necessary after the HTDHT procedure to achieve optimum performance. This is discussed later. With regard to the change in lignin size, the micromorphologies of the dry lignin powder and the SLEs were investigated by scanning electron microscopy (SEM). As we observed, the dry lignin powder was in the form of irregular agglomerates with a micrometer size [Figure 3(a)]. However, as shown in Figure 3(b–e), the lignin was well dispersed throughout the ENR matrix. Moreover, because of the huge internal friction between the lignin particles and lignin–rubber matrix, the particle size of lignin seemed to be smaller with increasing lignin loading. Eventually, the size of the lignin was reduced to about 250 nm. Simultaneously, the interface between the lignin and the ENR matrix was very obscure; this indicated a great compatibility between them.

Curing Behavior

The curing progress of the SLEs at 180°C was elucidated by the S' versus time curve shown in Figure 4(a); this also revealed the dependence of the curing reaction on $[L]$. Usually, the slope of the S' versus time curve represents the curing rate.[12] Obviously, the lignin-filled ENR exhibited a higher S' compared to the pure ENR. Moreover, the curing rate of the SLEs was higher with increasing $[L]$. These results indicate that the SLEs had a higher crosslinking density with increasing $[L]$ and curing time. This was very consistent with the results from the NMR measurements, as listed in Table I. We attributed this to the fact that the crosslinking density of the SLEs was practically dependent on the ring-opening extent of the epoxy groups in ENR, and the increase in $[L]$ improved the reaction probability with the epoxy groups and resulted in improvements in the reaction rate and crosslinking density.

As we know, an increase in S' is proportional to the crosslinking density. The change in S' during the curing progress is mainly associated with the ring-opening reaction.[11,12] If we assumed that the change in S' was directly proportional to the ring-opening reaction between lignin and ENR, the curing rate of the reaction could be written as follows:

$$\frac{dS'}{dt} = C\left(-\frac{d[L]}{dt}\right) = Ck[E]^m[L]^n \quad (1)$$

Equation (1) can be also written in the form of

$$\ln\left(\frac{dS'}{dt}\right) = \ln Ck[E]^m + n\ln[L] \quad (2)$$

where C is a proportionality constant, k is the reaction rate constant, $[E]$ is the epoxide concentration, t is the curing time and m and n are the respective orders of the reactants.

For a given formulation, the first term on the right side of eq. (2) can be considered a constant at the initial reaction stage with a maximum slope, and the plot of $\ln(dS'/dt)_{max}$ versus $\ln [L]_0$, where $[L]_0$ is the initial lignin concentration, should yield a straight line with a slope of n. Figure 4(b) shows their

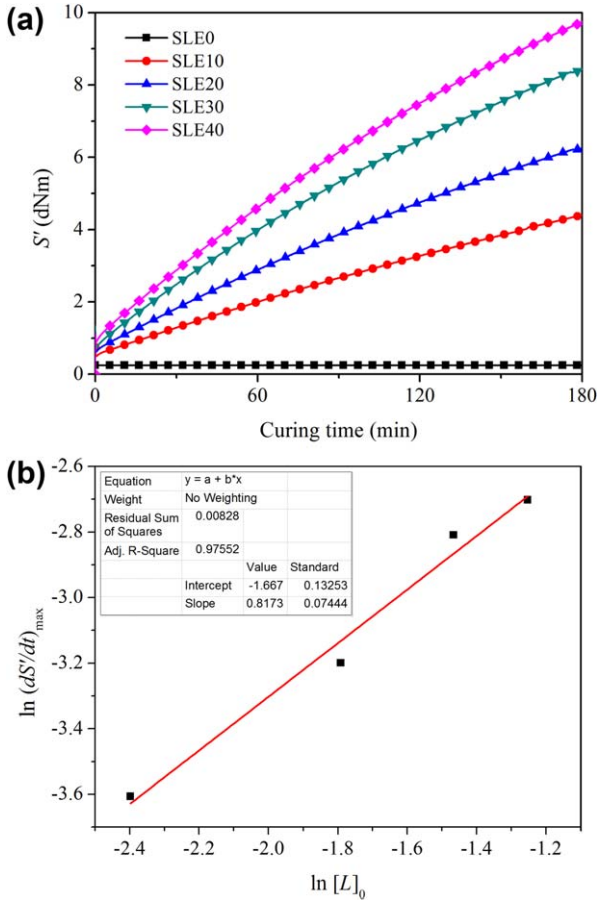

Figure 4. (a) Representative curing curves of SLE0, SLE10, SLE20, SLE30, and SLE40. (b) $\ln(dS'/dt)_{max}$ as a function of $[L]_0$ for the SLEs cured at 180°C and corresponding fitting curve. [Color figure can be viewed in the online issue, which is available at wileyonlinelibrary.com.]

relationship and the linear fitting curve, which gives an n of 0.817. Unlike other reactions of ENR with acids[7] and amines,[11,12] the reaction order n slightly deviated from 1; this was ascribed to the fact that the reaction between lignin and ENR belonged to a solid-phase reaction.

Tensile Properties

Because the optimum curing time of the SLEs could not be directly deduced from the curing curves of the SLEs at 180°C for 3 h, we simultaneously investigated the effect of the curing times (0.5, 1, 2, and 3 h) and $[L]$ on the tensile properties. The comparison in the tensile properties of the pure ENR and all of the SLEs cured at different times is shown in Figure 5. We observed that the tensile strength markedly increased with increasing $[L]$ and curing time up to a curing time of 3 h. Similarly, there was a gradual increase in the 100% modulus, which was also proportional to $[L]$ and the curing time. However, the elongation at break showed an opposite tendency. These phenomena could be viewed as a result of the increase in the crosslinking density of the SLEs. In an appropriate crosslinking density range, elastomer materials can form a homogeneous network structure, which can improve the tensile strength and modulus and decrease the rupture elongation with increasing crosslinking density.[28] However, overcuring will lead to a serious decrease in the mechanical properties because of stress concentration or a decreased strain-induced crystallization ability. In this study, with the inclusion of 40-phr lignin and curing for 2 h, the tensile strength of the SLEs was optimal and was almost 40-fold that of pure ENR. Beyond 2 h, the tensile properties of the SLEs, except SEL10, dramatically decreased. This was attributed to the fact that the crosslinking densities of SLE20, SLE30, and SLE40 were exorbitant after 3 h of curing; this resulted in an inhomogeneous network structure and stress concentration. However, the tensile strength of SLE10 increased slightly with increasing curing time. This may have been due to the weak confinement effect of lignin toward ENR at low $[L]$, which could not form effective stress transfer or an overcured network structure. Hence, the mechanical properties of the SLEs depended not only on the extent of the crosslinking reaction between lignin and ENR but also on $[L]$. The reinforcement mechanism of the SLE system is discussed in the following text.

Table I. Crosslinking Density ($\times 10^{-5}$ mol/cm^3) of the SLEs Cured at 180°C for Different Times

	Curing time (h)			
Sample	0.5	1	2	3
SLE10	6.81	8.62	10.03	11.36
SLE20	8.62	9.62	10.19	12.30
SLE30	8.86	10.10	10.60	13.11
SLE40	9.15	10.14	11.18	13.86

Dynamic Mechanical Properties

The viscoelastic behavior of a filled polymer under dynamic loading conditions can reveal the microstructure and interfacial interactions of the composites.[29] DMA is often used to study the viscoelastic characterizations and relaxations of a polymer

Table II. Correlative Parameters Obtained from a Cole–Cole Plot for the Pure ENR and the SLEs

Sample	E_G	E_R	θ_R	θ_G	$h = 2\theta_R/\pi$	$k = 2\theta_G/\pi$
SLE0	2109.2	2.023	56.16	20.52	0.624	0.228
SLE10	2422.6	2.884	55.89	20.25	0.621	0.225
SLE20	3406.3	3.513	54.18	19.08	0.602	0.212
SLE30	3938.0	4.085	54.09	17.28	0.601	0.192
SLE40	4687.6	4.198	53.46	12.87	0.594	0.143

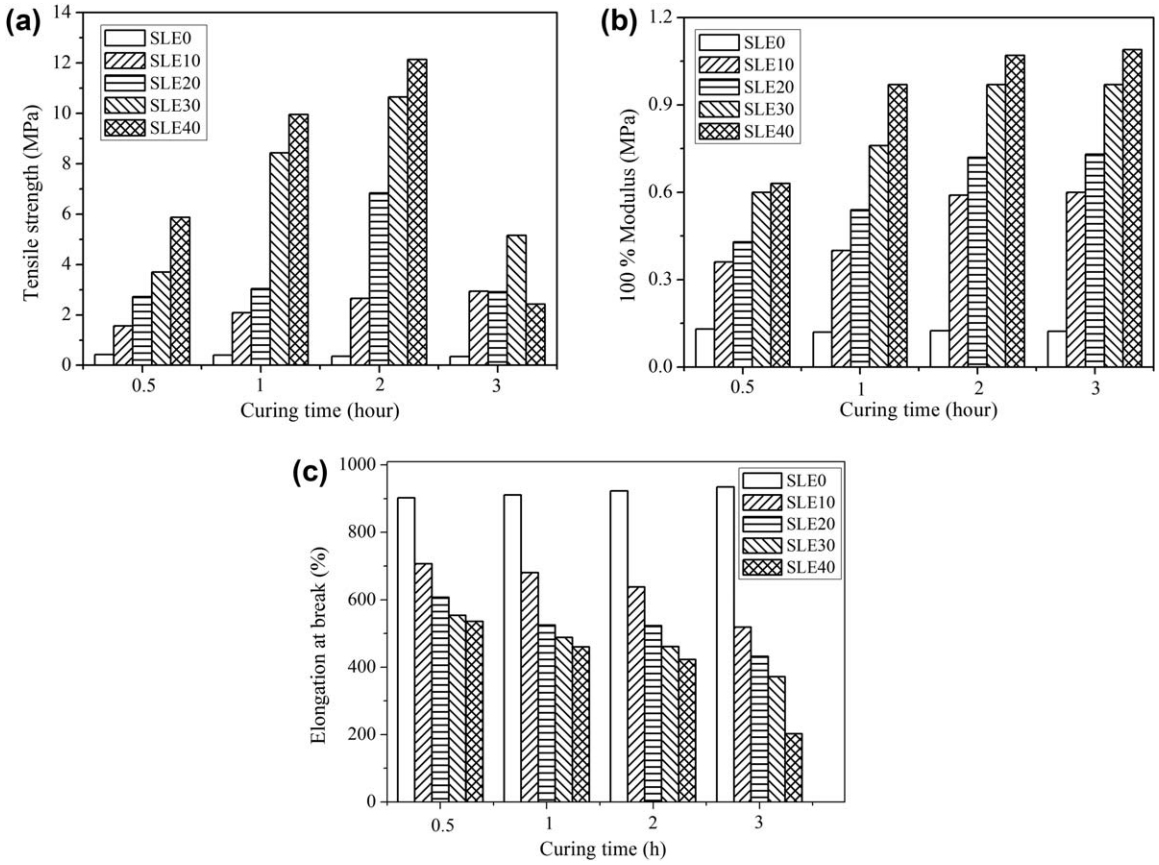

Figure 5. Tensile properties of the pure ENR and the SLEs cured at 180°C for different times: (a) tensile strength, (b) 100% modulus, and (c) elongation at break.

and its composites. The dynamic mechanical properties as a function of the temperature for the pure ENR and the SLEs after 2 h of curing are shown in Figure 6. As shown in Figure 6(a), the storage modulus (E') of the SLEs increased with increasing [L] in the entire observed temperature range. The results clearly show that the addition of lignin into the ENR matrix resulted in a remarkable increase in the stiffness of the material; this indicated the reinforcing effect of lignin. Specifically, E' of SLE40 in the glassy phase was almost two times higher that of pure ENR.

The loss tangent (tan δ) values of the samples that represent the damping characteristics are shown in Figure 6(b). Obviously, the pure ENR presented double peaks located at −51.3 and −39.9°C, respectively. However, the damping peak of the SLEs became one and gradually shifted to a higher temperature; this accompanied a considerable reduction in the tan δ peak height with increasing [L]. In particular, SLE20, SLE30, and SLE40 exhibited a higher increase in T_g compared to SLE10; this indicated a stronger confinement effect when [L] was greater than 10 phr, as shown in Figure 6(c). There seemed to be a percolation threshold between 10 and 20-phr lignin for the saltation of T_g. This may have depended on the difference in the distances between lignin particles in the ENR matrix and the effective thickness of the lignin–ENR matrix interphase, namely, whether the motion of all of the polymer chain segments could be restricted by fillers.[30] If all of the polymer chains were crosslinked by lignin, the translational flow and disentanglement flow of polymer chains will be prevented; this remarkably improved the T_g of the polymer compared to that of an incompletely crosslinked one.[31] Therefore, we could reasonably deduce that the ENR molecules of the SLEs with the inclusion of more than 10-phr lignin were completely crosslinked; this could form homogeneous networks to transfer external stress. No obvious variation in T_g of SLE10 compared with that of pure ENR indicated that not all of the chain segments of ENR could be restricted by lignin via covalent bonding. This further confirmed that the SLE10 could not form an effective crosslinking network at low [L]; this was in agreement with the inconspicuous increase in the mechanical properties of SLE10. On the basis of the previous analyses, this difference in the crosslinking networks of the SLEs was used to explain why the tensile strength of the SLEs with the inclusion of more than 10-phr lignin was better than that of SLE10 when the curing time was less than 3 h.

The relaxation of the polymer chains at the glass transition can be explained by molecular modeling for the deformation of an amorphous polymer near its T_g. This model has been applied to describe the influence of fillers on molecular restriction in amorphous, semicrystalline polymers and composites.[32] Hence, the complex modulus (E^*) can be expressed by

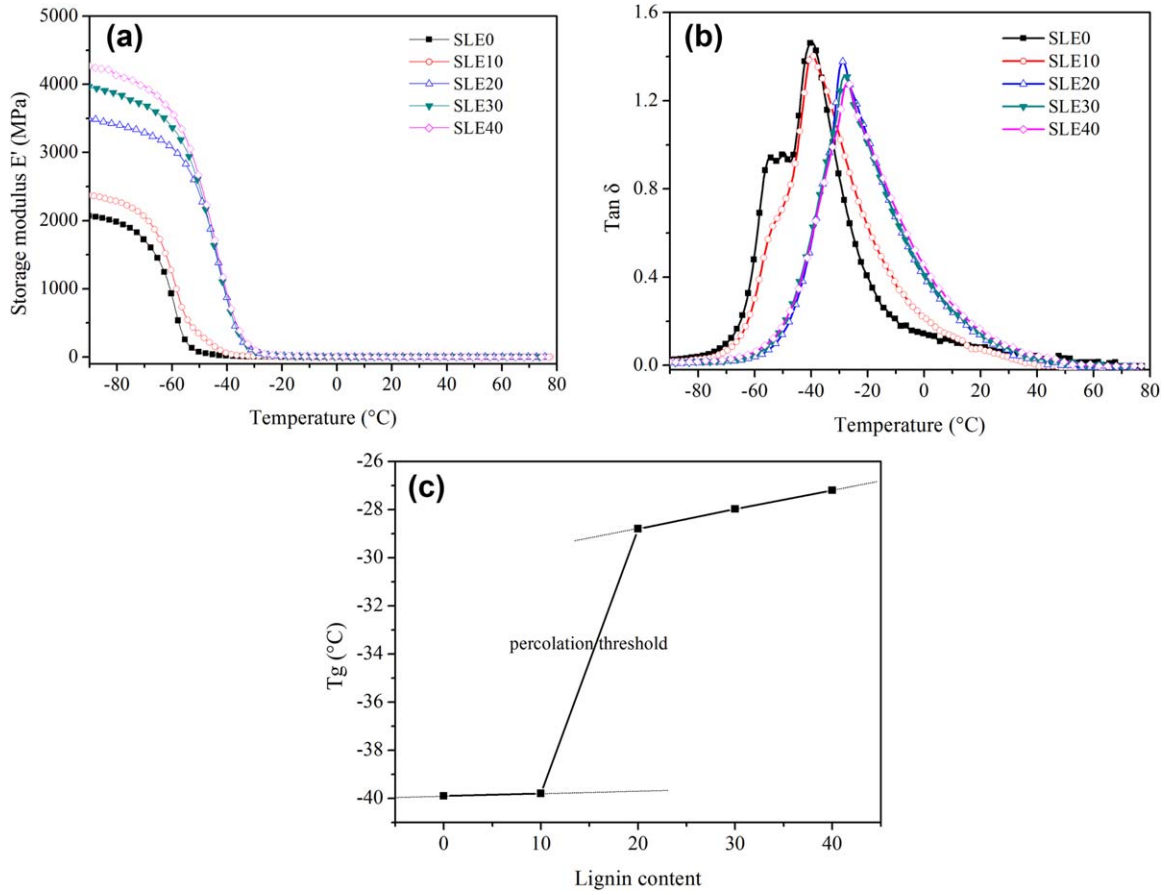

Figure 6. (a) E' versus temperature for the pure ENR and the SLEs after 2 h of curing. (b) Tan δ versus temperature for the pure ENR and the SLEs after 2 h of curing. (c) T_g of the SLEs as a function of $[L]$. A saltant elevation of T_g is indicated. [Color figure can be viewed in the online issue, which is available at wileyonlinelibrary.com.]

$$E^* = E_R + \frac{E_G - E_R}{1 + H(i\omega\tau)^{-h} + (i\omega\tau)^{-k}} \quad (3)$$

where E_G and E_R are the moduli of the polymer in the rubbery and glassy states, respectively; ω is the angular frequency; τ is the relaxation time at the glass transition; and i is an imaginary number ($\sqrt{-1}$). The parameter k ($0 < k < 1$) is consistent with the local motional ability of the chains, and h ($0 < k < h < 1$) is related to the presence of junction points (i.e., inclusions or chemical and/or physical crosslinks) hindering the molecular motion on a large scale. H is a function of k and h.

The correlative parameters in eq. (3) were determined from a Cole–Cole plot (Figure 7) obtained by the plotting of E' versus the loss modulus E''. h and k were obtained from the slopes of the Cole–Cole diagrams and corresponded respectively to lower and higher temperatures; that is, they were obtained from the angles between the tangent and the E' axis (θ_G and θ_R, respectively). E_G and E_R were obtained by the extension of this tangent onto the E' axis to lower and higher temperatures, respectively. The method for determining each of these parameters was explained in a previous literature.[32]

The parameter values obtained for the SLE systems are given in Table I. Both the k and h values decreased with increasing $[L]$. Here, k decreased from 0.288 to 0.143, and h decreased from 0.624 to 0.594. The decreases in these parameters resulted from the reduction in the segmental mobility of the polymer chain and the increased junction points of the ENR macromolecules caused by lignin curing. The results were in accordance with the reduction in the damping peak and the increase in T_g found

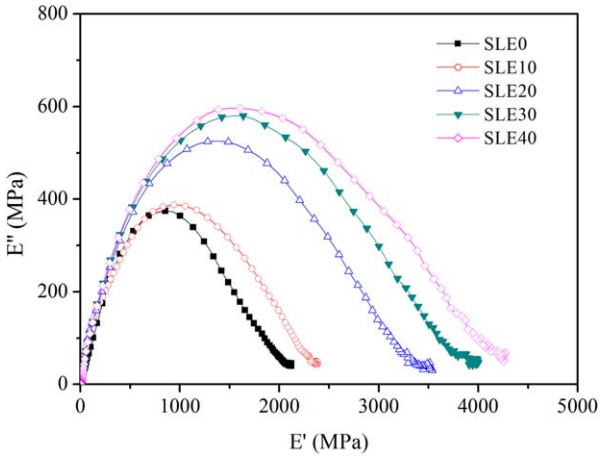

Figure 7. Cole–Cole plot of E' versus E'' for the pure ENR and the SLEs. [Color figure can be viewed in the online issue, which is available at wileyonlinelibrary.com.]

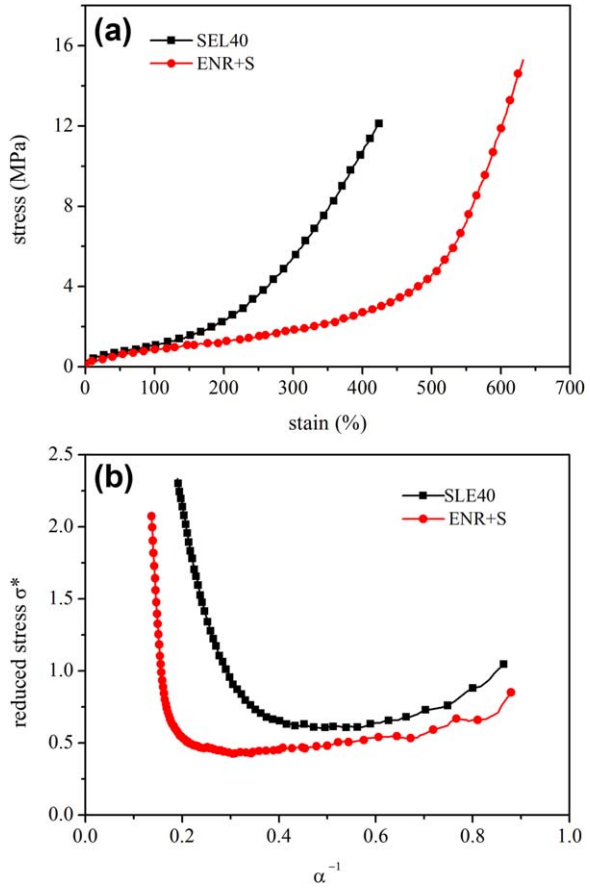

Figure 8. (a) Typical stress–strain curves of SLE40 after 2 h of curing at 180°C and sulfur-vulcanized pure ENR WITH a semi-efficient vulcanization system at 143°C. (b) Mooney–Rivlin plots of SLE40 and sulfur-vulcanized pure ENR. [Color figure can be viewed in the online issue, which is available at wileyonlinelibrary.com.]

from DMA. Also, they further confirmed the strong interfacial adhesion between lignin and ENR demonstrated by SEM.

Reinforcement Mechanism of the SLE Systems

As discussed previously, the mechanical properties of the SLEs mainly depended on the following two factors: [L] and crosslinking degree. At low [L], the SLEs could not form an effective crosslinking network to transfer stress; this resulted in a poor tensile strength. The increased crosslinking density of ENR with increasing [L] to some extent could improve the tensile properties. However, beyond a critical crosslinking level, the SLEs underwent a terrible deterioration in the tensile properties. This was ascribed to the stress concentration or inhibition of strain-induced crystallization. Therefore, the reinforcement mechanism of the SLEs needs further investigation. To resolve the issue, we compared the tensile properties of the SLEs and the pure ENR cured by a semi-efficient vulcanization system. Figure 8(a) shows the typical stress–strain curves of SLE40 and the sulfur-vulcanized ENR. SLE40 exhibited a higher modulus than the sulfur-vulcanized ENR at the same deformation; this indicated a higher stiffness. Moreover, the rupture elongation of SLE40 was significantly shorter than that of the sulfur-vulcanized ENR.

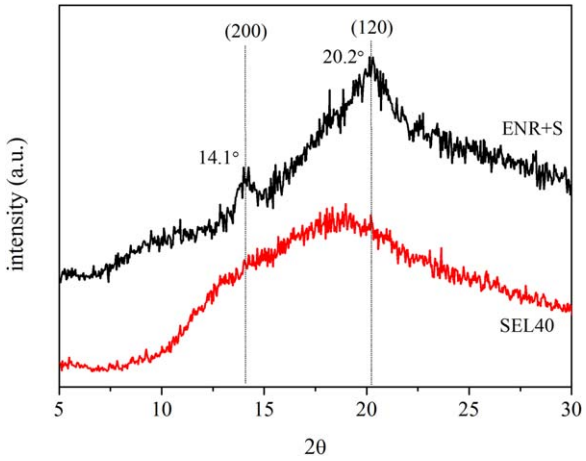

Figure 9. XRD patterns of the SEL40 and sulfur-vulcanized pure ENR (both stretched at $\lambda = 3.5$). [Color figure can be viewed in the online issue, which is available at wileyonlinelibrary.com.]

These results were attributed to the rigid network structure formed by the ring-opening reaction between lignin and ENR.

In addition, we were able to reveal other interesting features of the elastomeric networks by plotting the reduced stress [$\sigma^* = \sigma/(\alpha - \alpha^{-2})$], where σ is the nominal stress, defined as the force divided by the undeformed cross-sectional area, and α is the extension ratio, defined as the ratio of the final length of the sample in the direction of stretching to the initial length before deformation] against the reciprocal of α [Figure 8(b)]. This representation was suggested by the Mooney–Rivlin equation:[33,34]

$$\sigma^* = 2C_1 + 2C_2\alpha^{-1} \quad (4)$$

where $2C_1$ and $2C_2$ are constants that are independent of α. In the case of sulfur-vulcanized ENR with a 25 mol % epoxidation level, the strain-induced crystallization could be still observed because of the very uniform microstructure of the polymer chains and the rearrangement of the stretchable sulfur network.[35] This was responsible for the large and abrupt increase in σ^* observed at deformations approaching the maximum extensibility. This effect corresponded to a self-toughening of the elastomer because the crystallites acted as additional crosslinks in the network, strain amplifiers, and to some extent, filler particles. For SLE40, at low deformations, a slight decrease in the modulus was attributed to the Payne effect. Then, SLE40 exhibited an upturn in the modulus at smaller deformations than those of the sulfur-vulcanized ENR; this was attributed to the limited chain extensibility of short chains bridging neighboring filler particles.[34] Whether the strain-induced crystallization at large deformations contributed to the upturns for both samples, the crystal structure of the two samples at an elongation of $\lambda = 3.5$ was investigated by XRD.

As shown Figure 9, the sulfur-vulcanized ENR exhibited two distinct reflections. Analogous to the strain-induced crystallization of pure natural rubber,[36] the diffraction peaks at $2\theta = 14.1$ and 20.2° were assigned to the (200) and (120) plane reflections, respectively, of crystallites formed by ENR macromolecules. For SLE40, no obvious diffraction peaks were observed,

Table III. Comparison of the Tensile Properties of ENR Cured by Different Compounds

	Lignin-cured ENR	Amine-cured ENR[11]	Acid-cured ENR[7]	PLA[a]/glycol copolymer-cured ENR	Sulfonated EPDM[b]-cured ENR[37]
Tensile strength (MPa)	12.1	1.9	~5.0	6.0	0.3
Elongation at break (%)	422	410	690	407	1055

[a] PLA: Polylactic acid.
[b] EPDM: Ethylene-Propylene-Diene Monomer.

but only an amorphous halo was present; this indicated that there was no strain-induced crystallization in SLE40. Hence, we deduced that the reinforcement effect on the SLEs originated from the lignin as a reinforcing filler to bear stress rather than the crystallites formed by strain-induced crystallization.

It was noteworthy that the tensile strength of SLE40 was still slightly lower than that of the sulfur-vulcanized ENR, although it was reinforced by the loading of lignin. However, this strength was much better than that of other acid-cured, amine-cured, or polymer-cured[6,37] ENR systems, as shown in Table III. Moreover, for the same volumes of rubber products, the usage amount of the ENR matrix could be substantially reduced by filling such a large amount of lignin. In earlier publications, self-crosslinkable ENR blends could be reinforced by filling with nanofillers such as carbon black[12] or silica.[13] Therefore, for our investigated lignin/ENR systems, a further improvement in the mechanical properties was achieved with the following two approaches: (1) a reduction in the size of lignin to nanometers and (2) the incorporation of other reinforcing fillers into the SLE systems. These two approaches will be studied in our future work. Additionally, we predict that the SLEs have a superior aging resistance compared with sulfur-cured ENR because of their ability to scavenge free radicals of phenolic hydroxyls in lignin[21] and the consumption of epoxy groups in ENR by lignin.[7]

CONCLUSIONS

SLEs were prepared through an HTDHT procedure followed by postcuring at 180°C. The increase in the Haake S' verified the ring-opening reaction between the lignin and ENR. Morphological observation showed a homogeneous dispersion of lignin with a submicrometer size of about 250 nm in the ENR matrix and a great interfacial compatibility between them. The curing curves showed that the crosslinking degree and reaction rate increased with the addition of lignin. The optimum tensile strength of the SLEs could be achieved by the loading of 40-phr lignin and curing for 2 h. The DMA results showed that there was a percolation threshold between 10- and 20-phr lignin for the saltant elevation of T_g; this also demonstrated strong interactions between the lignin and ENR. From a comparison of the stress–strain curves of the SLEs and sulfur-vulcanized ENR, we deduced that the network structure formed via the ring-opening reaction was more rigid than that of the sulfur-vulcanized ENR; this hindered the strain-induced crystallization of the polymer chains; this was also verified by XRD. Therefore, the reinforcement effect on the SLEs mainly originated from lignin.

ACKNOWLEDGMENTS

The authors gratefully acknowledge the National Natural Science Foundation of China for its financial support (contract grant number U1134005/L04).

REFERENCES

1. Davies, C. K. L.; Wolfe, S. V.; Gelling, I. R.; Thomas, A. G. *Polymer* **1983**, *24*, 107.
2. Tanrattanakul, V.; Wattanathai, B.; Tiangjunya, A.; Muhamud, P. *J. Appl. Polym. Sci.* **2003**, *90*, 261.
3. Johnson, T.; Thomas, S. *Polymer* **1999**, *40*, 3223.
4. Rajasekar, R.; Nayak, G. C.; Malas, A.; Das, C. K. *Mater. Des.* **2012**, *35*, 878.
5. Sharif, N.; Mohamad, Z.; Hassan, A.; Wahit, M. *J. Polym. Res.* **2012**, *19*, 1.
6. Nguyen, T. H.; Tangboriboonrat, P.; Rattanasom, N.; Petchsuk, A.; Opaprakasit, M.; Thammawong, C.; Opaprakasit, P. *J. Appl. Polym. Sci.* **2012**, *124*, 164.
7. Pire, M.; Norvez, S.; Iliopoulos, I.; Le Rossignol, B.; Leibler, L. *Polymer* **2010**, *51*, 5903.
8. Chang, Y.; Mishra, J. K.; Cheong, J.; Kim, D. *Polym. Int.* **2007**, *56*, 694.
9. Zhang, P.; Huang, G.; Qu, L.; Nie, Y.; Weng, G. *J. Appl. Polym. Sci.* **2012**, *125*, 1084.
10. Pire, M.; Norvez, S.; Iliopoulos, I.; Le Rossignol, B.; Leibler, L. *Polymer* **2011**, *52*, 5243.
11. Hashim, A. S.; Kohjiya, S. *Polym. Gels Networks* **1994**, *2*, 219.
12. Hashim, A. S.; Kohjiya, S. *J. Polym. Sci. Part A: Polym. Chem.* **1994**, *32*, 1149.
13. Hashim, A. S.; Kohjiya, S.; Ikeda, Y. *Polym. Int.* **1995**, *38*, 111.
14. Vainio, U.; Maximova, N.; Hortling, B.; Laine, J.; Stenius, P.; Simola, L. K.; Gravitis, J.; Serimaa, R. *Langmuir* **2004**, *20*, 9736.
15. Gosselink, R. J. A.; Abächerli, A.; Semke, H.; Malherbe, R.; Käuper, P.; Nadif, A.; van Dam, J. E. G. *Ind. Crops Prod.* **2004**, *19*, 271.

16. Košíková, B.; Gregorová, A.; Osvald, A.; Krajčovičová, J. *J. Appl. Polym. Sci.* **2007**, *103*, 1226.
17. Gregorová, A.; Košíková, B.; Moravčík, R. *Polym. Degrad. Stab.* **2006**, *91*, 229.
18. Botros, S. H.; Eid, M. A. M.; Nageeb, Z. A. *J. Appl. Polym. Sci.* **2006**, *99*, 2504.
19. Simionescu, C. I.; Rusan, V.; Macoveanu, M. M.; Cazacu, G.; Lipsa, R.; Vasile, C.; Stoleriu, A.; Ioanid, A. *Compos. Sci. Technol.* **1993**, *48*, 317.
20. Feldman, D.; Banu, D.; Natansohn, A.; Wang, J. *J. Appl. Polym. Sci.* **1991**, *42*, 1537.
21. Jiang, C.; He, H.; Jiang, H.; Ma, L.; Jia, D. M. *eXPRESS Polym. Lett.* **2013**, *7*, 480.
22. Sirianni, A. F.; Puddington, I. E. *U.S. Pat. 3,984,362* (**1976**).
23. Kubo, S.; Kadla, J. F. *Biomacromolecules* **2005**, *6*, 2815.
24. Hatakeyama, H.; Tsujimoto, Y.; Zarubin, M. J.; Krutov, S. M.; Hatakeyama, T. *J. Therm. Anal. Calorim.* **2010**, *101*, 289.
25. Dence, C. W.; Lin, S. Y. Methods in Lignin Chemistry; Springer: Berlin, **1992**.
26. Irvine, G. M. *Wood Sci. Technol.* **1985**, *19*, 139.
27. Hatakeyama, T.; Hirose, S.; Hatakeyama, H. *Makromol. Chem.* **1983**, *184*, 1265.
28. Heinrich, G.; Straube, E.; Helmis, G. Rubber Elasticity of Polymer Networks: Theories; Springer: Berlin, **1988**; Vol. *85*, p 33.
29. Kader, M.; Kim, K.; Lee, Y. S.; Nah, C. *J. Mater. Sci.* **2006**, *41*, 7341.
30. Robertson, C. G.; Rackaitis, M. *Macromolecules* **2011**, *44*, 1177.
31. Ndoni, S.; Vorup, A.; Kramer, O. *Macromolecules* **1998**, *31*, 3353.
32. Bergeret, A.; Alberola, N. *Polymer* **1996**, *37*, 2759.
33. Joly, S.; Garnaud, G.; Ollitrault, R.; Bokobza, L.; Mark, J. E. *Chem. Mater.* **2002**, *14*, 4202.
34. Bokobza, L. *Macromol. Symp.* **2001**, *169*, 243.
35. Davies, C. K. L.; Wolfe, S. V.; Gelling, I. R.; Thomas, A. G. *Polymer* **1983**, *24*, 107.
36. Toki, S.; Sics, I.; Ran, S.; Liu, L.; Hsiao, B. S.; Murakami, S.; Senoo, K.; Kohjiya, S. *Macromolecules* **2002**, *35*, 6578.
37. Manoj, N. R.; De, P. P.; De, S. K.; Peiffer, D. G. *J. Appl. Polym. Sci.* **1994**, *53*, 361.